6-30-2014

Quantifying the local density of optical states of nanorods by fluorescence lifetime imaging

Jingjing Liu
Purdue University, Birck Nanotechnology Center, Bindley Bioscience Center, jjliu@purdue.edu

Xunpeng Jiang
Purdue University, Birck Nanotechnology Center, China Agricultural University

Satoshi Ishii
Purdue Univeristy, Birck Nanotechnology Center, National Institution of Information and Communication Technology Japan

V. M. Shalaev
Birck Nanotechnology Center and School of Electrical and Computer Engineering, Purdue University, shalaev@purdue.edu

Joseph Irudayaraj
Purdue University, Birck Nanotechnology Center, Bindley Bioscience Center, josephi@purdue.edu

Quantifying the local density of optical states of nanorods by fluorescence lifetime imaging

2014 New J. Phys. 16 063069

(http://iopscience.iop.org/1367-2630/16/6/063069)

New Journal of Physics
The open access journal at the forefront of physics
Deutsche Physikalische Gesellschaft DPG | IOP Institute of Physics

Quantifying the local density of optical states of nanorods by fluorescence lifetime imaging

Jing Liu[1,2], Xunpeng Jiang[1,3], Satoshi Ishii[2,4,5], Vladimir Shalaev[2,4] and Joseph Irudayaraj[1,2]

[1] Department of Agricultural and Biological Engineering, and Bindley Bioscience Center, Purdue University, West Lafayette, IN 47907, USA
[2] Birck Nanotechnology Center, Purdue University, West Lafayette, IN 47907, USA
[3] College of Engineering, China Agricultural University, Beijing 100083, People's Republic of China
[4] School of Electrical and Computer Engineering, Purdue University, West Lafayette, IN 47907, USA
[5] Advanced ICT Research Institute, National Institute of Information and Communications Technology, Kobe, 651-2492, Japan
E-mail: josephi@purdue.edu

Received 10 February 2014, revised 9 May 2014
Accepted for publication 22 May 2014
Published 30 June 2014

New Journal of Physics **16** (2014) 063069

doi:10.1088/1367-2630/16/6/063069

Abstract

In this paper, we demonstrate a facile far-field approach to quantify the near-field local density of optical states (LDOS) of a nanorod using CdTe quantum dot (QD) emitters tethered to the surface of the nanorods as beacons for optical read-outs. The radiative decay rate was extracted to quantify the LDOS; our analysis indicates that the LDOS of the nanorod enhances both the radiative and non-radiative decay of QDs, particularly the radiative decay of QDs at the end of a nanorod is enhanced by 1.17 times greater than that at the waist, while the nonradiative decay was enhanced uniformly over the nanorod. To the best of our knowledge, our effort constitutes the first to map the LDOS of a nanostructure via the far-field method, to provide clarity on the interaction mechanism between emitters and the nanostructure, and to be potentially employed in the LDOS mapping of high-throughput nanostructures.

Keywords: LDOS, fluorescence lifetime imaging, quantum dots, far-field

Interactions between emitters and the environment, which focus on the modulation of spontaneous emission and understanding of their optical as well as the electronic scattering and propagation characteristics, is the heart of nano-optics and photonics [1–5]. The spontaneous emission [6] is inherently determined by the dipole transition momentum of the emitters, and externally influenced by the surrounding local density of optical states (LDOS). Theoretically the LDOS is defined as the imaginary part of Green's function [7] and generally includes all possible optical modes, which not only affects the optical properties of the surroundings [8–14], but also has a significant influence on the chemical reactions that occur in the vicinity [15, 16]. Engineering a spontaneous emission by manipulating the LDOS has significant implications in the fields of energy, communication, and quantum optics; to effectively manipulate the LDOS and control the emission of spontaneous emitters metallic surfaces [1–4, 8, 9], photonic crystals [17–19], nanostructures [9, 13, 14, 20–27], and quite recently hyperbolic metamaterials [10–12], have been introduced.

Due to the importance of LDOS on the engineering of spontaneous emissions, detection and quantification of LDOS can promote our understanding of nano-optics. Recently emitters have been used as probes to report on the LDOS. Random drop-casting emitters were often used to detect the LDOS [5, 8, 12], but the uncertainty in the position of the emitters cannot guarantee the accuracy of detection. The break through method to detect the LDOS of a single nanostructure was proposed in 2002 by controlling the probes via nanopositioning [27, 28, 30–33]. It can either directly quantify the coupled photonic intensity through the nano-sized fiber tip, or extensively record the time-resolved emission from the well-characterized probes. However, this technique is relatively complex to implement, iterative probing/scanning increases the risk of scanning reversibility; and more critically, the introduction of the near-field probe gives rise to a strong external local gradient in the electric field [7]. Cathodoluminescence (CL), which collects luminescence upon excitation by electron beams, is an intact technique used to detect the LDOS in the far-field beyond the diffraction limit, but this approach can only detect the radiative modes of the LDOS, and poses high restrictions on the environment and operation [29]. To the best of our knowledge, a simple and robust method to detect and quantify the near-field local photonic density of single nanoscale structures via use of a far-field technique has not been attempted.

In this paper, we propose a facile platform to map the LDOS of single nanostructures without the intricacies involved in nanopositioning required in the near-field. Cadmium Telluride (CdTe) quantum dots (QDs) as spontaneous emitters were conjugated to the surface of gold nanorods (AuNRs) by chemical modification. The distance between the QDs and the AuNRs could be controlled by a thin layer of silica at nanometer precision. The LDOS of the AuNR is deduced by recording and analyzing the spontaneous decay of the QDs, and the radical LDOS of the AuNRs can be detected by controlling the distance between the QDs and the AuNRs with a thin layer of silica. The method presented will lead to a fast and convenient means to detect and quantify the photonic density for use in the design of photonic structures.

As discussed above, light emission is determined by the transition dipole momentum of the emitters and the LDOS. The radiative decay rate, γ_{Rad}, of a quantum emitter in a medium can be described by [7, 19]:

$$\gamma_{Rad} = \frac{2\omega_0}{3\hbar\varepsilon_0} |\mu|^2 \rho_\mu(r, \omega_0), \text{ with } \rho_\mu(r, \omega_0) = \frac{6\omega_0}{\pi c^2}\left[n_\mu \cdot \mathrm{Im}\left\{\vec{G}(r, r; \omega_0)\right\} \cdot n_\mu\right] \quad (1)$$

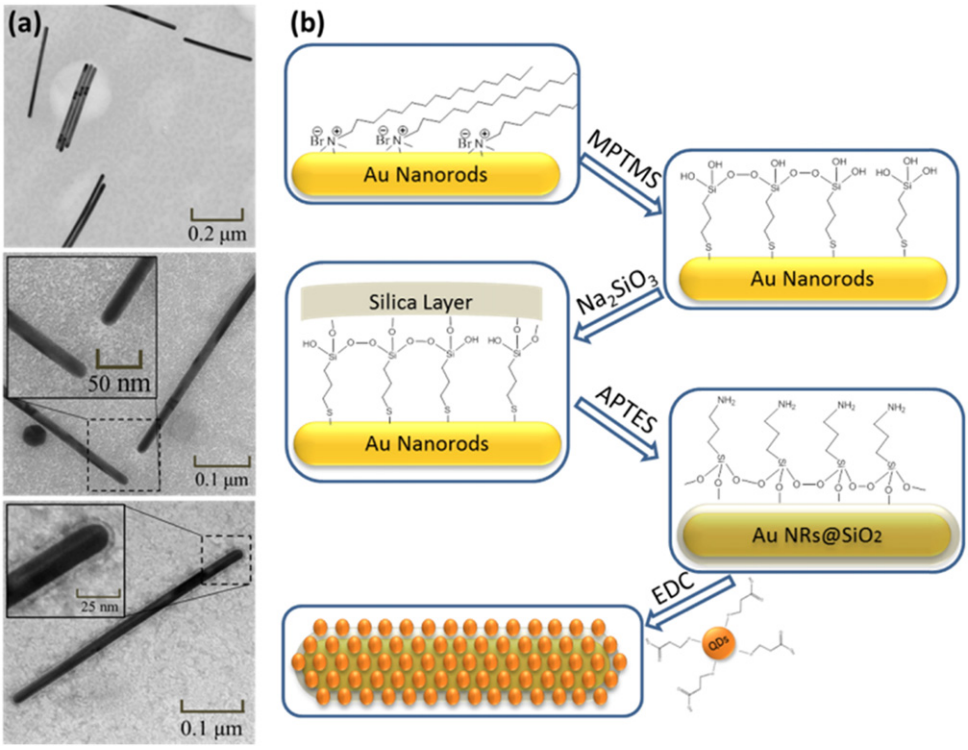

Figure 1. Biofunctionalization of AuNRs with QDs. (a) Transmission electron microscopy (TEM) images of AuNRs (top), AuNRs coated with silica (middle), and silica-coated AuNRs coated with QDs (bottom). (b) Conceptual description of the biofunctionalization procedure. (Structures are schematic and not to scale).

where ω_0 is the excitation frequency, $\hbar$ is Planck's constant, ε_0 is the dielectric constant in a vacuum, μ is the transition dipole momentum of the emitter, $\rho_\mu(r, \omega_0)$ denotes the projected LDOS, c is the speed of light in a vacuum, n_μ denotes the unit vector of μ; Im $\left\{\vec{\vec{G}}(r, r; \omega_0)\right\}$ is the imaginary part of Green's function that defines the LDOS. Therefore, we found that by obtaining γ_{Rad} one can deduce the LDOS.

In our experiment, we selectively locate the spontaneous emitters a few nanometers away from the AuNR. As shown in figure 1, a layer-by-layer coating method was applied by chemical conjugation, with AuNRs constituting the inner core, silica as the intermediate spacer layer, and QDs as the outer illumination/detection layer. Briefly, in our experiment we start with the synthesis of AuNRs that are ~400 nm long and ~40 nm wide, fabricated by the three-step seeding method reported by Murphy and co-workers [34–36]. A thin layer of silica was coated onto the surface of the AuNRs [37]. Finally, water soluble QDs were conjugated onto the silica layer to complete the material construction [25].

Spontaneous emissions of QDs are recorded by confocal fluorescence lifetime imaging microscopy (FLIM), which does not involve nanopositioning control and has the ability to record the signal in the far-field. The system, as shown in figure 2(a), is developed based on a commercial platform, Picoquant TimeHarp 200, which is a confocal scanning microscopy with an integrated time-correlated single photon counting (TCSPC) module. A picosecond pulsed laser beam at a 467 nm wavelength with a repetition frequency of 10 MHz was delivered onto

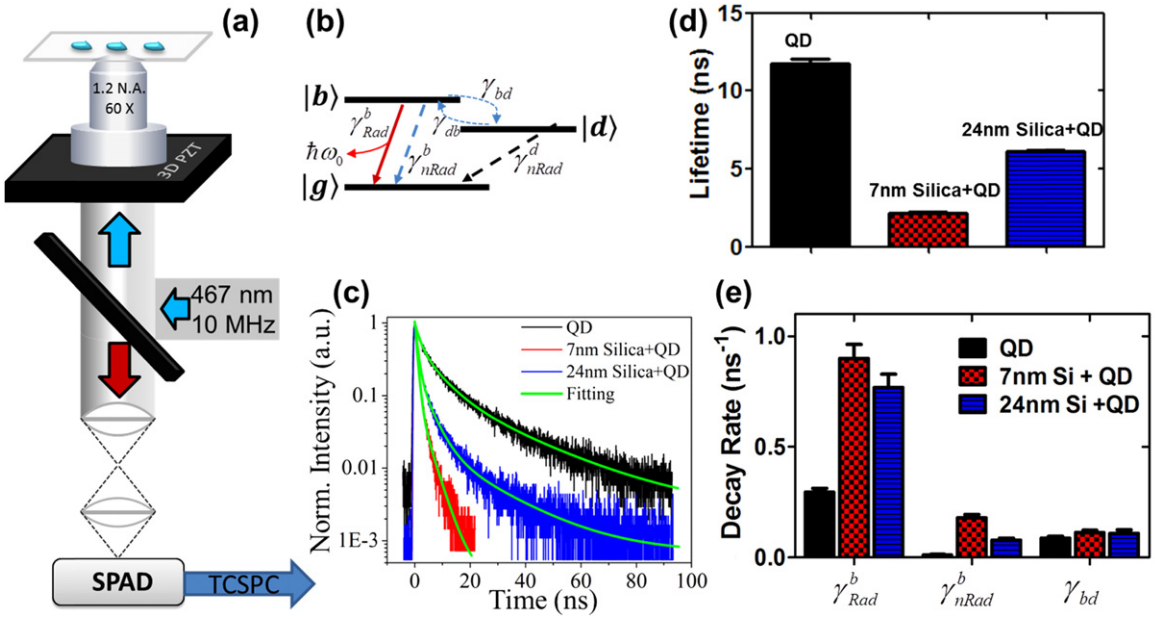

Figure 2. Schematic of the measurement unit and analyses concepts. (a) Experimental design of the instrument. (b) Exciton levels of the CdTe QDs. (c) Time correlated single photon counting (TCSPC) decay of the fluorescence signal collected from the QDs described in (b), 'QD' presents the case when a QD is in vacuum; '7 nm Silica + QD' ('24 nm silica + QD') presents the case when a QD is coated onto the AuNRs, isolated by a 7 nm (24 nm) silica layer. (d) The average lifetime of QDs on the surface of the AuNRs fitted from (c). (e) Analysis of the decay behavior of QDs from (c) calculated using equations (2) and (3).

the sample by a water-immersion objective (OLYMPUS UPLANAPO, 60x/1.2), leading to the lateral spatial resolution of the system at around 200 nm. The excited fluorescence emission was collected by the same objective and filtered by a dichroic mirror, a 50 μm pinhole was used to reject the background noise and the out-of-focus fluorescence, and the signal was filtered again by a band-pass filter (585–645 nm, Omega) before entering the single photon avalanche photodiodes (SPAD) (SPCM-AQR-14, PerkinElmer Inc.). Details of the instrument and data acquisition can be found in [38] and [39].

Before enumerating the spontaneous decay of QDs around the NR, briefly we discuss the fine energy structure of CdTe QDs [40, 41]. The exciton level of a CdTe QD can be simplified as a three-level system, consisting of a bright state, dark state, and the ground state (figure 2(b)). The spontaneous decay of CdTe QDs can step through multiple pathways. The bright state $|b\rangle$ can relax to the ground state $|g\rangle$ via either radiative or nonradiative decay at the rate γ^b_{Rad} and γ^b_{nRad}, respectively; meanwhile $|b\rangle$ could transition to the dark state $|d\rangle$ with a spin-flip rate γ_{bd}. The radiative transition between the dark state and ground state is forbidden, while the nonradiative recombination of electrons and holes is possible at the rate γ^d_{nRad}; and in addition, $|d\rangle$ can also flip to $|b\rangle$ at the rate of γ_{db}, where $\gamma_{bd} = e^{\delta_{bd}/k_BT}\gamma_{db}$ [19, 40, 42], δ_{bd} is the splitting energy between $|b\rangle$ and $|d\rangle$ ($\sim$100 μeV) [40, 42], k_B is the Boltzmann constant, and T is the experimental temperature ($\sim$300 K). Here we take an approximation $\gamma_{bd} \cong \gamma_{db}$ since $k_BT \gg \delta_{bd}$;

furthermore, γ_{nRad}^{d} can be approximated to γ_{nRad}^{b} due to the small δ_{bd} compared with the energy between the excited and ground states (~2 eV) [43], and this approximation has been experimentally proven valid by measuring the γ_{nRad}^{b} and γ_{nRad}^{d} of QDs in a known LDOS [43, 44].

Since the fluorescence emitted from a QD is collected in a steady state, the exciton population $N_b(t)$ of the bright state $|b\rangle$ can be deduced from the population equation [19, 42]

$$N_b(t) = A_1 e^{-\gamma_1 t} + A_2 e^{-\gamma_2 t} \tag{2}$$

with

$$\gamma_1 = \gamma_{nRad}^{b} + \frac{1}{2}\gamma_{Rad}^{b} + \gamma_{db} + \sqrt{\left(\gamma_{db}\right)^2 + \left(\gamma_{Rad}^{b}\right)^2/4}$$

$$\gamma_2 = \gamma_{nRad}^{b} + \frac{1}{2}\gamma_{Rad}^{b} + \gamma_{db} - \sqrt{\left(\gamma_{db}\right)^2 + \left(\gamma_{Rad}^{b}\right)^2/4}$$

$$A_1 = \frac{N_b(0)}{2}\left(1 + \frac{\gamma_{Rad}^{b}}{\gamma_1 - \gamma_2}\right) - N_d(0)\frac{\gamma_{db}}{\gamma_1 - \gamma_2}$$

$$A_2 = \frac{N_b(0)}{2}\left(1 - \frac{\gamma_{Rad}^{b}}{\gamma_1 - \gamma_2}\right) + N_d(0)\frac{\gamma_{db}}{\gamma_1 - \gamma_2}. \tag{3}$$

Here $N_b(0)$ and $N_d(0)$ are the initial exciton populations of $|b\rangle$ and $|d\rangle$, respectively; for the weak pumping, $N_b(0)$ and $N_d(0)$ can be set as $N_b(0) = N_d(0) = 0.5$ [19, 42] (assuming that the overall population of excited states is 1).

The fluorescence signal recorded by the SPAD is then processed in the TCSPC mode by the SymPhoTime software (Picoquant, Germany), where all the TCSPC curves (figure 2(c)) were fitted via the least-square fitting by

$$I(t) = a_0 \gamma_{Rad}^{b} N_b(t) \tag{4}$$

and one can obtain values of parameters γ_1, γ_2, A_1 and A_2 (R^2 of all fittings are in the range [0.995, 1]). The average lifetime of the sample was obtained from $\tau_{avg} = \left(A_1(1/\gamma_1)^2 + A_2(1/\gamma_2)^2\right)/\left(A_1(1/\gamma_1) + A_2(1/\gamma_2)\right)$ (the intensity-averaged lifetime); the radiative decay rate γ_{Rad}^{b}, nonradiative decay rate γ_{nRad}^{b}, and spin-flip rate γ_{bd} were calculated using equations (2) and (3). All results are shown in figures 2(c)–(e). It should be noted that generally the inverse of the lifetime equals the 'total' decay rate which summarizes γ_{Rad}^{b} and γ_{nRad}^{b} [19], therefore in our report we extracted γ_{Rad}^{b} from the total spontaneous decay and applied it to calculate the LDOS.

Figure 2(c) shows the experimental measurements and theoretical fitting of time-resolved spontaneous emissions from QDs coated on the AuNRs with different silica thicknesses, and the statistics of calculated average lifetimes is presented in figure 2(d). The QDs show different lifetimes as the distances between the AuNRs and the QDs vary, which was estimated as in [25]. The QDs on the AuNRs with the thinnest silica layer (7 nm) exhibit the least lifetime, ~2.17 ns; while the QDs on the AuNRs with a thicker silica layer and on a coverslip yield much larger lifetimes, ~6.11 ns for QDs on a 24 nm silica layer and ~11.74 ns for QDs on a coverslip (without a silica layer). This is because the closer the emitter approximates to AuNRs, the more effective coupling between excited emitters and

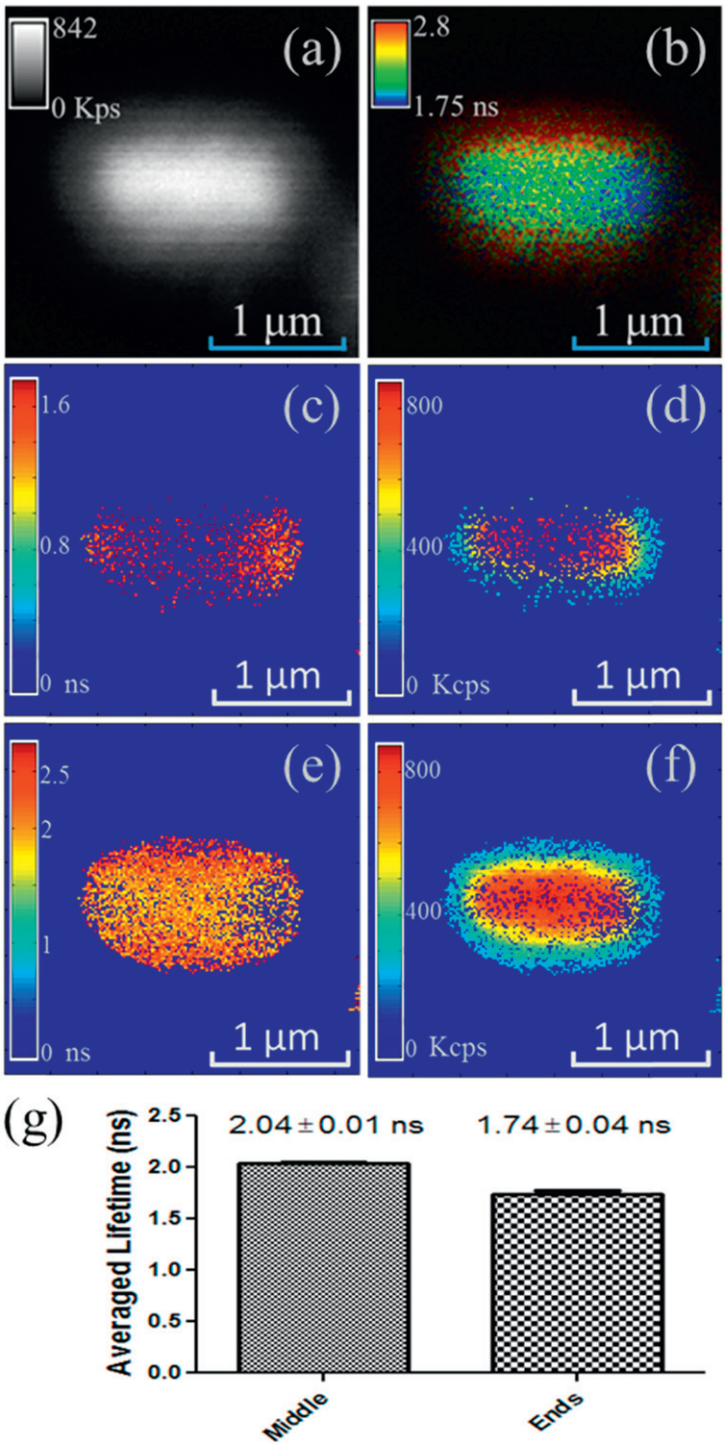

Figure 3. Lifetime distribution of QDs on a AuNR surface coated with a 5 nm layer of silica. (a) Intensity image of QDs on AuNRs; (b) lifetime mapping of QDs on AuNRs; lifetime (c) and intensity (d) image of QDs with a lifetime smaller than 1.8 ns; separated lifetime (e) and intensity (f) image of QDs with a lifetime greater than 1.8 ns; (g) average lifetime of QDs at the waist and ends of the AuNR. Unit in (a), (d) and (f): 'Kcps' represents a thousand counts per second.

LDOS of the AuNRs occurs. Furthermore, by solving equation (3) with the parameters fitted from the TCSPC decay curves in figure 2(c), the respective radiative decay rate and nonradiative decay rate of QDs can be obtained, as compared in figure 2(e). First, γ_{Rad}^{b}, γ_{nRad}^{b}, and γ_{bd} of the QDs on the glass coverslip are $0.2545 \pm 0.018\,\mathrm{ns}^{-1}$, $0.0119 \pm 0.002\,\mathrm{ns}^{-1}$, and $0.1028 \pm 0.008\,\mathrm{ns}^{-1}$, suggesting the high quantum yield of QDs on a coverslip and a lifetime of ~4 ns (in agreement with the calculated amplitude-averaged lifetime, $\tau_{avg}^{Amp} = \left(A_1(1/\gamma_1) + A_2(1/\gamma_2)\right)/\left(A_1 + A_2\right)$. Note: in this paper, the default average lifetime is the intensity-averaged lifetime), which indicates the robustness of our calculation. As a contrast, γ_{Rad}^{b} $\left(\gamma_{nRad}^{b}\right)$ of QDs on AuNRs with 7 and 24 nm gaps is enhanced significantly to $0.8999 \pm 0.063\,\mathrm{ns}^{-1}$ ($0.1788 \pm 0.015\,\mathrm{ns}^{-1}$) and $0.7684 \pm 0.066\,\mathrm{ns}^{-1}$ ($0.0821 \pm 0.009\,\mathrm{ns}^{-1}$), respectively. It is found that γ_{Rad}^{b} is enhanced by ~3–3.5 times for QDs on AuNRs than that for QDs on a coverslip, but the γ_{nRad}^{b} is enhanced as much as fifteen times (this enhancement factor was called 'inhibit factor' in [19]. The radiative enhancement generally comes from the coupled localized surface plasmon resonance of AuNRs, and this enhancement reduces with the increased gap between emitters and AuNRs, as observed here (γ_{Rad}^{b} varies from $0.2545\,\mathrm{ns}^{-1}$ (no AuNRs), to $0.8999\,\mathrm{ns}^{-1}$ (7 nm gap with AuNRs), and to $0.7684\,\mathrm{ns}^{-1}$ (24 nm gap with AuNRs)). While for the non-radiative decay rate, the enhancement comes not only from the coupled localized plasmon resonance, but also from the surface energy transfer (SET) procedure, which is dominant when the gap between emitter and AuNRs is smaller than 10 nm [45]. The SET-induced enhanced nonradiative decay rate also decreases with the increased gap between emitters and AuNRs (γ_{nRad}^{b} varies from $0.0119\,\mathrm{ns}^{-1}$ (no AuNRs), to $0.1788\,\mathrm{ns}^{-1}$ (7 nm gap with AuNRs), and to $0.0821\,\mathrm{ns}^{-1}$ (24 nm gap with AuNRs)).

Although figure 2 shows that the LDOS of a metal nanostructure has a strong coupling with spontaneous emitters that are held in close proximity to the nanomaterial, the results represent an average lifetime of emitters on multiple AuNRs, typically used in other related studies [25]. Note that the characterization and quantification of the LDOS of an individual AuNR have rarely been reported. Our work allows one to map the LDOS of AuNRs by quantifying the spontaneous decay of the quantum emitters.

QDs were coated onto AuNRs (~400 nm) and separated by a 5 nm-thick silica layer (shown in figure 1(a)). Figure 3 shows the fluorescence intensity and lifetime images of QDs on AuNR on the coverslip. It is clear from the FLIM image (figure 3(b)) that the QDs at the two ends of the nanorod have smaller lifetimes compared to the QDs at the waist of the nanorod, while the intensity image (figure 3(a)) does not show the enhancement at the ends or waist. The difference in lifetime is further clarified in figures 3(c)–(f), where distributions of photons with different lifetimes are depicted. Figures 3(c) and (d) are the FLIM and intensity distribution maps of photons with lifetimes in the range between 0–1.8 ns, while (e) and (f) denote images with lifetimes greater than 1.8 ns. Our analysis indicates that QDs at the ends of the nanorods have a smaller lifetime, which is about 1.74 ± 0.04 ns, while the average lifetime of QDs at the waist of the nanorod is about 2.04 ± 0.01 ns. This comparison is shown in figure 3(g).

The results obtained describe the lifetime distribution of spontaneous emitters on a metal nanostructure, which can be specifically assigned to the coupling of the spontaneous decay of QDs with the LDOS of the metal nanostructure. By analyzing the time-resolved spontaneous decay, one can assess the influence of the LDOS on the radiative and nonradiative decay rate of QDs on a single metallic nanostructure.

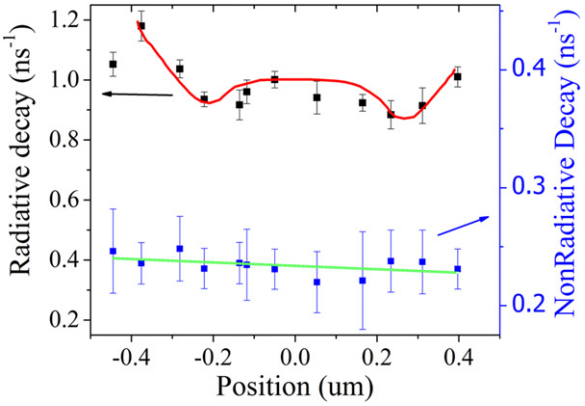

Figure 4. Radiative (black) and nonradiative (blue) decay rate of QD on a AuNR (coated with a 5 nm layer of silica) with respect to the length of the AuNR. Black: radiative decay, red: theoretical fitting from figure 5. Blue: Nonradiative decay, green: theoretical fitting.

As discussed above, the time resolved fluorescence decay curve contains contributions from both the radiative and nonradiative decay behavior of emitters, although the previous reports have just focused on the time-resolved spectroscopy to obtain information on the average lifetime [27]. It is important to extract each of these decay rates for a comprehensive map of effects of the LDOS and to clarify the role of the decay behavior with respect to light–matter interaction. Equations (2), (3) and (4) were applied to calculate γ^{b}_{Rad} and γ^{b}_{nRad} of QDs at different positions on the AuNR. As shown in figure 4, the radiative decay rate γ^{b}_{Rad} suggests maximum values at the two ends of the AuNR, a medium value at the waist of the NR, and a minimum value at the position between the ends and waist. Our results clearly show that, on a AuNR, the radiative decay of QDs is more pronounced at the ends than at the waist. While for the nonradiative decay rate, there is less variation in the values obtained at the different positions, suggesting that the nonradiative decay rate is equally enhanced on the AuNRs.

This is the first experimental quantification of the near-field LDOS of a nanorod using far-field methods. It is worth noting here that we use a chemical conjugation method to precisely localize QDs 5 nm apart from the AuNR, and to quantify the LDOS 5 nm from the AuNR. Considering the uniformity of the distribution of QDs on the AuNR, the emission behavior exactly reveals the near-field LDOS of a AuNR. By varying the thickness of the silica layer between QDs and AuNRs, one can obtain a detailed 3D near-field LDOS distribution of the AuNR. While for the nano-positioning technique, it is difficult to precisely control the nano-probe to as close as 5 nm from the AuNRs; in addition, the LDOS of the AuNR would be dramatically changed if a nano-sized probe is approaching it.

The experimental results were validated by simulation of the LDOS using the full-wave numerical simulation based on the finite-element method with the software COMSOL (COMSOL Inc.). The structural parameters were extracted from the TEM images shown in figure 1, and the dielectric constants were obtained from an online tool from nanoHUB.org [46]. From equation (1) we know that the LDOS is proportional to the imaginary part of Green's function; in addition, we deduce Green's function from $E(r, \omega) = \mu_0 \omega^2 G(r, r_0, \omega) p$ [32], where $E(r, \omega)$ is the electronic field around the NR, and p is the dipole of the QD. Figure 5

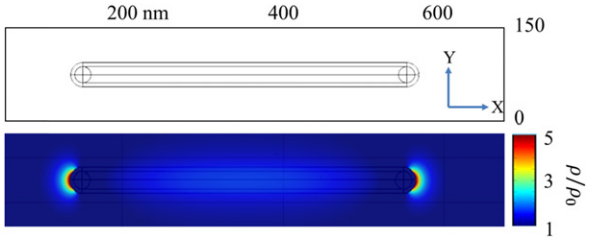

Figure 5. Numerical simulation of LDOS on a nanorod under laser irradiation on the x-y plane. The thickness of the silica layer is 5 nm. The ends reveal intense states.

shows the LDOS maps of a AuNR based on our simulation. The LDOS profiles at the x-y and x-z plane both qualitatively show that the enhanced LDOS was observed at the two ends of the nanorods compared to the values at the waist, which is in agreement with the LDOS map shown in figures 3 and 4. In addition, simulation also suggests that the positions of minimum LDOS are found in the vicinities of the ends of AuNRs (compare the color bar of the simulation result); correspondingly at that position the minimum enhancement of the radiative decay rate was observed (figure 4), although the resolution of figure 4 is limited by the microscopy.

To summarize, we have demonstrated a new platform to detect the LDOS of a nanoscale metallic structure in the far-field, which can potentially be used for single molecule sensing. QDs were covalently attached to the surface of AuNRs via chemical conjugation for evaluation and their interacting distances with the NR were controlled at nanometer resolution. Fluorescence lifetime imaging of the QDs on the NR indicates that the LDOS at the ends of the nanostructure were greater than their effect at the waist. Our analytical study also shows the influence of LDOS on the radiative decay and nonradiative decay of QDs on the NR, and was confirmed by numerical simulation. The developed methods can be widely applied to evaluate the LDOS of other nano-structures and meta-materials to promote the design and development of novel photonic and quantum devices.

Acknowledgments

The authors would like to acknowledge funding support from the National Science Foundation (grant # 1294315). JL would like to acknowledge the SIRG assistantship from the Purdue Center for Cancer Research (funded by NIH). SI would like to acknowledge financial support from the Japan Society for the Promotion of Science (JSPS) Postdoctoral Fellowships for Research Abroad. Gururaj Naik, Nuri Damayanti, and Jingjing Liu are acknowledged for the helpful discussion on the theory and simulations.

References

[1] Ford G W and Weber W H 1984 *Phys. Report* **113** 195
[2] Amos R M and Barnes W L 1997 *Phys. Rev.* B **55** 7249
[3] Lakowicz J R, Shen Y, D'Auria S, Malicka J, Fang J, Gryczynski Z and Gryczynski I 2002 *Ana. Biochem.* **301** 261
[4] Lakowicz J R and Geddes C D 2002 *J. Fluo.* **12** 121
[5] Ruppin R and Martin O J F 2004 *J. Chem. Phys.* **121** 11358
[6] Purcell E M 1946 *Phys. Rev.* **69** 681

[7] Novotny L and Hecht B 2006 *Principles of Nano-Optics* (Cambridge: Cambridge University Press)
[8] Krachmalnicoff V, Castanie E, Wilde Y D and Carminati R 2010 *Phys. Rev. Lett.* **105** 183901
[9] Anger P, Bharadwaj P and Novotny L 2006 *Phys. Rev. Lett.* **96** 113002
[10] Bakker R M, Drachev V P, Liu Z, Yuan H, Pedersen R H, Boltasseva A, Chen J, Irudayaraj J, Kildishev A V and Shalaev V M 2008 *New J. Phys.* **10** 125022
[11] Jacob Z, Kim J Y, Naik G V, Boltasseva A, Narimanov E E and Shalaev V M 2010 *Appl. Phys.* B **100** 215
[12] Krishnamoorthy H N S, Jacob Z, Narimanov E E, Kretzschmar I and Menon V M 2012 *Science* **336** 205
[13] Lee J, Govorov A O, Dulka J and Kotov N A 2004 *Nano Lett.* **4** 2323
[14] Chang D E, Sorensen A S, Hemmer P R and Lukin M D 2006 *Phys. Rev. Lett.* **97** 053002
[15] Zijlstra P, Paulo P M R and Orrit M 2012 *Nat. Nanotechnology* **7** 379
[16] Zhou X, Andoy N M, Liu G, Choudhary E, Han K, Shen H and Chen P 2012 *Nat. Nanotechnology* **7** 237
[17] Lodahl P, van Driel A F, Nikolaev I S, Irman A, Overgaag K, Vanmaekelbergh D and Vos W L 2004 *Nature* **430** 654
[18] Noda S, Fujita M and Asano T 2007 *Nat. Photonics* **1** 449
[19] Wang Q, Stobbe S and Lodahl P 2011 *Phys. Rev. Lett.* **107** 167404
[20] Akimov A V, Mukherjee A, Yu C L, Chang D E, Zibrov A S, Hemmer P R, Park H and Lukin M D 2007 *Nature* **450** 402
[21] Fedutik Y, Temnov V V, Schops O, Woggon U and Artemyev M V 2007 *Phys. Rev. Lett.* **99** 136802
[22] Ming T, Zhao L, Yang Z, Chen H, Sun L, Wang J and Yan C 2009 *Nano Lett.* **9** 3896
[23] Wei H, Ratchford D, Li X, Xu H and Shih C 2009 *Nano Lett.* **9** 4168
[24] Gramotnev D K and Bozhevolnyi S 2010 *Nat. Photonics* **4** 83
[25] Li X, Kao F, Chuang C and He S 2010 *Opt. Express* **18** 11335
[26] Curto A G, Volpe G, Taminiau T H, Kreuzer M P, Quidant R and van Hulst N F 2010 *Science* **329** 930
[27] Frimmer M, Chen Y and Koenderink A F 2011 *Phys. Rev. Lett.* **107** 123602
[28] Chicanne C, David T, Quidant R, Weeber J C, Lacroute Y, Bourillot E, Dereux A, des Frances G C and Girard C 2002 *Phys. Rev. Lett.* **88** 097402
[29] Knight M W, Liu L, Wang Y, Brown L, Mukherjee S, King N S, Everitt H O, Nordlander P and Halas N J 2012 *Nano Lett.* **12** 6000
[30] Ropp C, Cummins Z, Nah S, Fourkas J T, Shapiro B and Waks E 2013 *Nat. Commun.* **4** 1447
[31] Hoogenboom J P, Sanchez-Mosteiro G, des Francs G C, Heinis D, Legay G, Dereux A and van Hulst N F 2009 *Nano Lett.* **9** 1189
[32] Krachmalnicoff V, Cao D, Caze A, Castanie E, Pierrat R, Bardou N, Collin S, Carminati R and De Wilde T 2013 *Opt. Express* **21** 11536
[33] Frimmer M and Koenderink A F 2013 *Phys. Rev. Lett.* **110** 217405
[34] Jana N R, Gearheart L and Murphy C J 2001 *J. Phys. Chem.* B **105** 4065
[35] Yu C, Varghese L and Irudayaraj J 2007 *Langmuir* **23** 9114
[36] Yu C and Irudayaraj J 2007 *Anal. Chem.* **79** 572
[37] Obare S O, Jana N R and Murphy C J 2001 *Nano Lett.* **1** 601
[38] Chen J and Irudayaraj J 2010 *Anal. Chem.* **82** 6415
[39] Liu J and Irudayaraj J 2013 *Opt. Express* **21** 27063
[40] Van Driel A F, Allan G, Delerue C, Lodahl P, Vos W L and Vanmaekelbergh D 2005 *Phys. Rev. Lett.* **95** 236804
[41] Schlegel G, Bohnenberger J, Potapova I and Mews A 2002 *Phys. Rev. Lett.* **88** 137401
[42] Lin S D, Fu Y J and Cheng C 2012 *Opt. Express* **20** 19850
[43] Stobbe S, Johansen J, Kristensen P T, Hvam J M and Lodahl P 2009 *Phys. Rev.* B **80** 155307
[44] Johansen J, Julsgaard B, Stobbe S, Hvam J M and Lodahl P 2010 *Phys. Rev.* B **81** 081304(R)
[45] Dulkeith E, Morteani A C, Niedereichholz T, Klar T A, Feldmann J, Levi S A, van Veggel F C J M, Reinhoudt D N, Möller M and Gittins D I 2002 *Phys. Rev. Lett.* **89** 203002
[46] Ni X, Liu Z and Kildishev A V 2010 *PhotonicsDB: Optical Constants* http://nanohub.org/resources/PhotonicsDB doi:(10.4231/D3FT8DJ4J)